J. Fluid Mech. (1990), *vol.* 221, *pp.* 437–451
Printed in Great Britain

Buoyancy-induced Stokes flow in a wedge-shaped enclosure

By K. M. YU[1] AND M. W. NANSTEEL[2]

[1] Department of Mechanical Engineering and Applied Mechanics, University of Pennsylvania, Philadelphia, PA 19104, USA

[2] Department of Mechanical and Aerospace Engineering, Florida Institute of Technology, Melbourne, FL 32901, USA

The problem of buoyancy-induced Stokes flow in a sectorial region is addressed. Skew-symmetric flows are considered for wedge or opening angles of the sector in the range $0 < \alpha \leqslant \pi$. The basic structure and character of the motion are found to depend critically upon the relative dominance, near the sector vertex, of the particular solution of the system with respect to the leading eigenfunction. A simple criterion is developed for the appearance of eddies, such as those observed by Moffatt (1964), in the neighbourhood of the sector vertex. A calculation is carried out for the specific case of motion induced by different temperatures on the radial boundaries of the enclosure. It is found that corner eddies may be present in this circumstance for wedge angles in the range $126° \lesssim \alpha \lesssim 146°$. The eddying motion near the vertex is examined, in some detail, for the wedge angle $\alpha = 135°$. In the limiting case of $\alpha = \pi$, corresponding to a semicircular-shaped sector, the particular solution is found to exhibit singular behaviour. However, this singular nature is found to be spurious, as a bounded particular solution can be constructed with the aid of one of the eigensolutions. Results are given for no-slip and shear-free conditions on the circular boundary of the sector for the purpose of comparison.

1. Introduction

Fluid motions in which inertia effects are negligible have been widely studied. Interest in these Stokes flows is due, at least in part, to the linear form of the governing equations which yield, in many cases, closed-form solutions. Owing to the simple, explicit nature of these solutions they generally yield local information about the flow more readily than a full-scale numerical solution and hence they are often a good starting point for developing a clear physical understanding of a particular flow. Of special interest here are Stokes flows in the neighbourhood of a sharp corner. Such flows are particularly interesting because of the way in which local (near-the-corner) and far-field effects compete for dominance in the neighbourhood of the corner or vertex. This dominant behaviour near the vertex, of course, depends on the opening or wedge angle of the corner since larger opening angles allow greater opportunity for the physical processes far from the vertex to penetrate and influence the local behaviour. However, the dominant behaviour near the corner and hence the local flow structure also depends upon the specific nature of the local and far-field effects producing the motion. Moffatt (1964) describes several corner flows which are either driven by local effects such as prescribed boundary velocity at the vertex or by a disturbance located far from the corner. Locally driven flows are described by

a particular solution of the governing system, which in Moffatt's case satisfies inhomogeneous conditions on the radial boundaries corresponding to the prescribed boundary velocity. If the flow is driven by a disturbance in the far field, the flow is described by eigenfunctions of the homogeneous system. Moffatt (1964) pointed out that for some ranges of the wedge angle, α, these eigenfunctions could give rise to an infinite cascade of 'corner eddies' of diminishing size and circulation strength as distance from the vertex decreased. The eddy patterns, although independent of the nature of the far-field disturbance in a qualitative sense, require complete specification of the disturbance in order to determine their location and scale. Lugt & Schwiderski (1965) placed the results of Moffatt (1964) on a firm foundation by proving the completeness of the set of eigenfunctions under the condition that the fluid velocity vanishes at the vertex.

The formation of an infinite sequence of eddies near a boundary in a viscous fluid, although curious, is quite plausible. A useful physical interpretation for the formation of corner eddies in Stokes flow was given by Jeffrey & Sherwood (1980). Jeffrey & Sherwood note that Stokes flows dissipate the least amount of energy for a given set of boundary velocities (cf. Batchelor 1967, p. 227). Hence the eddies, which in a sense approximate rigid-body rotation, may be the preferred flow structure, i.e. the structure required in order to minimize the dissipation of mechanical energy. This interpretation is supported by the fact that corner eddies cease to exist (except perhaps under rather special circumstances) for corner angles α greater than some angle $\alpha = \alpha_1$, say. It would seem that less straining is required of a flow with open streamlines for larger corner angles so that beyond a certain angle $\alpha = \alpha_1$, eddies are less efficient in minimizing energy dissipation and hence do not appear.

Of course in any finite domain with the flow driven locally (near the vertex) the global solution for the resulting flow will be a superposition of the particular solution and the eigensolutions. In such a case the appearance of corner eddies depends on the relative dominance of the leading eigensolution with respect to the particular solution in the neighbourhood of the vertex as well as on the wedge angle α. Such a case was considered by Liu & Joseph (1977) in which the motion in a liquid-filled wedge-shaped trench was driven by a difference of temperature between the radial surfaces. The shape of the free liquid surface, which comprised the remaining boundary of the sector, was determined in the course of the analysis. The complete solution for the motion was found by utilizing the biorthogonal properties of the eigenfunctions. This procedure led to an explicit expression for the coefficients in the eigenfunction series. In the study of Liu & Joseph (1977) wedge angles were confined to the range $0 \leqslant \alpha \leqslant \frac{1}{2}\pi$ for which corner eddies do not appear in the flow even though corner eigenfunctions do. This is because in this range of α the particular solution (corresponding to the heating condition of Liu & Joseph) dominates the leading corner eigenfunction in the neighbourhood of the vertex.

Another interesting aspect of corner convection concerns the apparent singular behaviour of the particular integral of the Stokes equations which sometimes arises for certain isolated and distinct values of the corner angle α. This singular behaviour presents a paradox since little physical justification can be found for the unboundedness of the solution. This phenomenon arises in a number of different physical contexts. Sternberg & Koiter (1958) examine the stress distribution in an elastic wedge of opening angle α subjected to a couple which is concentrated at the vertex. The stress components are shown to be unbounded at all points in the wedge when the angle $\alpha = \alpha^* \approx 257°$. This problem is analogous to the cases of Stokes flow

discussed here since the stress components of Sternberg & Koiter (1958) are derived from a biharmonic function, i.e. the Airy stress function. Dempsey (1981) resolved the apparent paradox for $\alpha = \alpha^*$ by introducing more general stress functions which give rise to logarithmic stress singularities at the wedge vertex. More recently, Ting (1984) has obtained a uniformly valid solution which is bounded for α near α^* and reduces to Dempsey's result for $\alpha = \alpha^*$. Similar paradoxical behaviour arises for systems governed by Laplace or Poisson equations. Moffatt & Duffy (1980) examine Poiseuille flow in a duct whose cross-section has a sharp corner. In this circumstance the axial velocity, which satisfies a Poisson equation, exhibits singular behaviour (through the particular solution) for the corner angles $\alpha = \frac{1}{4}\pi$ and $\frac{3}{4}\pi$. Moffatt & Duffy resolve the singular behaviour at these critical angles by using appropriate components of the homogeneous solution to compensate for the singularity in the particular solution. Ting (1985) uses similar reasoning in order to resolve the singular stresses which arise in an elastic wedge subjected to uniform antiplane shear tractions for wedge angles of π and 2π. A similar approach will be shown to be of value in treating this paradoxical behaviour as it arises in the corner convection under study here.

In this paper we examine buoyancy-induced Stokes flow in a sectorial region for wedge angles α in the range $0 < \alpha \leqslant \pi$. We consider here skew-symmetric flows only since the underlying methodology is quite similar for symmetric motions in the sector. Simple criteria for the appearance of corner eddies are discussed. A specific example corresponding to isothermal heating and cooling of the radial boundaries of the sector is examined in detail. It is shown that this particular set of thermal conditions may result in corner eddies within the wedge angle range $126° \lesssim \alpha \lesssim 146°$. The detailed structure, location and scale of the corner eddies for the case $\alpha = 135°$ are examined. The singular nature of the particular solution that arises for $\alpha = \pi$ is resolved by superimposing an appropriate member of the eigenfunction series on the particular solution in order to compensate for the spurious singularity. Results for a zero velocity slip and also a shear-free condition on the circumferential boundary of the sector are discussed.

2. Analysis

Consider the fluid-filled circular sector of opening or wedge angle α and radius R shown in figure 1. Attention is focused here upon sectors with opening angle $0 < \alpha \leqslant \pi$. Note that the specific case $\alpha = \pi$ corresponds to an enclosure in the shape of a semicircular duct with a differentially heated floor section. It is expected that differential heating of the sector boundaries (the precise nature of which will be specified later) gives rise, at least in the neighbourhood of the vertex $\bar{r} = 0$, to a steady, laminar two-dimensional fluid motion. It is also assumed that physical properties such as kinematic viscosity ν, thermal diffusivity κ and expansion coefficient β are constant while changes in density ρ are small (and linear with temperature) and hence affect the motion only through the generation of buoyancy. If the boundary heating is not too strong, the present conditions suggest an increase in density along any circumferential path traversed in the direction of decreasing θ. Therefore an overall clockwise recirculation pattern should prevail in which more dense fluid descends along the boundary $\theta = -\frac{1}{2}\alpha$ and less dense fluid rises adjacent to the boundary $\theta = \frac{1}{2}\alpha$. However, it will be demonstrated later that this simple unicellular motion may not exist for certain heating conditions and opening angles α. In the case of a small driving temperature difference on the radial boundaries,

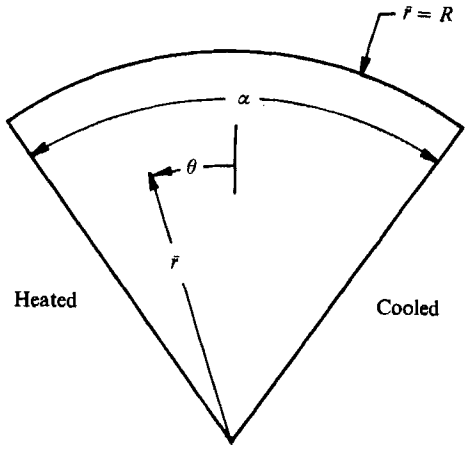

FIGURE 1. Fluid-filled sector of opening angle α.

circulation in the sector is weak and energy transfer, to lowest order, is dominated by conduction (see Liu & Joseph 1977) so that

$$\nabla^2 T = 0, \tag{2.1}$$

where fluid temperature $\bar{T}$ has been made dimensionless with an appropriate characteristic temperature difference γ,

$$T = (\bar{T} - \bar{T}_0)/\gamma,$$

and the subscript zero denotes a reference condition. It is demonstrated by Liu & Joseph (1977) that in this Stokes limit there exists in the sector a balance between pressure, viscous and buoyancy effects so that, in addition to

$$\nabla \cdot \boldsymbol{u} = 0, \tag{2.2}$$

fluid velocity is governed by

$$\nabla^2 \boldsymbol{u} - T(\boldsymbol{e}_0 \sin\theta - \boldsymbol{e}_r \cos\theta) - \nabla p = 0, \tag{2.3}$$

in which dimensionless fluid velocity $\boldsymbol{u}$, pressure p and radial coordinate r are defined in terms of their dimensional equivalents $\bar{\boldsymbol{u}}$, $\bar{p}$, and $\bar{r}$:

$$\boldsymbol{u} = \frac{\bar{\boldsymbol{u}}\nu}{g\beta\gamma R^2}, \quad p = \frac{\bar{p} + \rho_0 g \bar{r} \cos\theta}{\rho_0 g \beta \gamma R}, \quad r = \frac{\bar{r}}{R}.$$

It is important to note that even under arbitrary heating conditions a region in the neighbourhood of the sector vertex $r = 0$ can always be found in which the viscous-dominated results (2.1) and (2.3) apply.

Eliminating pressure from (2.3) and introducing the stream function ψ in order to satisfy (2.2),

$$u_r = \frac{1}{r}\frac{\partial \psi}{\partial \theta}, \quad u_\theta = -\frac{\partial \psi}{\partial r},$$

yields the following fourth-order equation for ψ:

$$\nabla^4 \psi = -\left(\sin\theta \frac{\partial T}{\partial r} + \frac{\cos\theta}{r}\frac{\partial T}{\partial \theta}\right), \tag{2.4}$$

where $\psi(r,\theta)$ must satisfy the conditions of impermeability and zero velocity slip on the boundaries of the sector

$$\psi(r, \pm\tfrac{1}{2}\alpha) = \frac{\partial\psi}{\partial\theta}(r, \pm\tfrac{1}{2}\alpha) = 0, \tag{2.5}$$

$$\psi(1,\theta) = \frac{\partial\psi}{\partial r}(1,\theta) = 0. \tag{2.6}$$

For given thermal conditions on the radial and circumferential boundaries, solution of (2.1) yields the right-hand side of (2.4) as a known function, $g(r,\theta)$ say, which serves to drive the flow in sector. The system (2.4)–(2.6) is identical to that governing the transverse deflection of a thin plate built-in at the edges and subjected to a pressure distribution on its surface which is proportional to $g(r,\theta)$. It is of interest to consider the general nature of solutions to (2.4). For instance, it seems physically reasonable to expect that under some circumstances, for example small α, the fluid motion near the sector vertex would be determined completely by heating conditions in the neighbourhood of $r = 0$. For larger opening angles it is reasonable to expect that the effect of far-field conditions may more easily penetrate into the vertex region and hence influence this local behaviour. This independence (for small r) of the remote geometry for small wedge angles was observed by Moffatt & Duffy (1980) in the case of Poiseuille flow through a straight duct whose cross-section has a sharp corner.

Equations (2.4) and (2.5) are satisfied by superposing a particular solution, ψ_p, which satisfies (2.4) and (2.5) with solutions satisfying the homogeneous form of (2.4) along with the conditions (2.5). The solutions are combined in such a manner that the condition of zero velocity on the circumferential boundary (2.6) is satisfied. For simplicity we consider here only the case of a stream function symmetric in θ, i.e. skew-symmetric flows in the nomenclature of Moffatt (1964) and Lugt & Schwiderski (1965). From (2.4), (2.5) and (2.6) it is evident that such flows correspond to thermal boundary conditions yielding even functions $g(r,\theta)$. Biharmonic functions corresponding to skew-symmetric motions are given by

$$\psi_\lambda = r^{\lambda+1}\left[\cos[(\lambda+1)\theta] - \frac{\cos[(\lambda+1)\tfrac{1}{2}\alpha]}{\cos[(\lambda-1)\tfrac{1}{2}\alpha]}\cos[(\lambda-1)\theta]\right]. \tag{2.7}$$

The parameter λ must satisfy the requirements

$$\sin\lambda\alpha = -\lambda\sin\alpha, \tag{2.8}$$

$$\mathrm{Re}(\lambda) > 0 \tag{2.9}$$

in order that (2.5) is satisfied and fluid velocity vanishes at the sector vertex, $r = 0$. It is demonstrated by Lugt & Schwiderski (1965) that the functions (2.7) with the λ determined by (2.8) form a complete set under the restriction (2.9). The sequence of eigenvalues λ_n corresponding to (2.8) has been discussed by Moffatt (1964), Lugt & Schwiderski (1965) and Liu & Joseph (1977). For wedge angles less than a value $\alpha_1 \approx 146°$ the λ_n form a countable infinity of complex-conjugate pairs. As α increases from α_1 to π the number of real solutions of (2.8) increases from one to infinity. When $\alpha = \pi$ all eigenvalues are real.

The full solution satisfying (2.4)–(2.6) is then

$$\psi = \psi_p + \sum_n A_{\lambda_n}\psi_{\lambda_n}, \tag{2.10}$$

where the constants A_{λ_n} are complex when λ_n is complex and are chosen so that the condition of zero velocity on the circumferential boundary (2.6) is satisfied. Since the stream function is real-valued, (2.10) may be simplified to

$$\psi = \psi_p + \sum_n \mathrm{Re}\{A_{\lambda_n} \psi_{\lambda_n}\}. \tag{2.11}$$

For opening angles less than α_1 the leading eigenvalue $\lambda_1 \equiv \lambda_{1r} + i\lambda_{1i}$ and the leading eigenfunction ψ_{λ_1} are complex. Since the solutions of (2.8) occur as conjugate pairs (for $\alpha < \alpha_1$) and since $\psi_{\bar{\lambda}_1} = \bar{\psi}_{\lambda_1}$ it follows from the reality of ψ that $A_{\bar{\lambda}_1} = \bar{A}_{\lambda_1}$. Therefore, the leading term in the summation of (2.11) is of the form

$$\mathrm{Re}\{A_{\lambda_1}\psi_{\lambda_1} + \bar{A}_{\lambda_1}\bar{\psi}_{\lambda_1}\} = -2|A_{\lambda_1} f_1(\theta)| r^{\lambda_{1r}+1} \sin(\lambda_{1i} \log r + \arg(2A_{\lambda_1} f_1(\theta)) - \tfrac{1}{2}\pi), \tag{2.12}$$

where

$$f_1(\theta) = \cos[(\lambda_1+1)\theta] - \frac{\cos[(\lambda_1+1)\tfrac{1}{2}\alpha]}{\cos[(\lambda_1-1)\tfrac{1}{2}\alpha]} \cos[(\lambda_1-1)\theta].$$

It is evident that the leading term (2.12) dominates the solution (2.11) near the sector vertex $r = 0$ provided

$$\psi_p = o[r^{\lambda_{1r}+1}], \quad r \to 0. \tag{2.13}$$

Whether or not (2.13) is satisfied depends on the opening angle α and on the thermal boundary conditions. It is of interest to note that along any radius in the sector the term (2.12) changes sign with unbounded frequency as the sector vertex is approached. This oscillatory nature was first noticed by Moffatt (1964), who interpreted the corresponding corner flow as an infinite sequence of eddies whose size and strength diminishes with decreasing r. It is also evident from (2.12) that the precise nature of this localized eddy sequence depends on conditions far from $r = 0$ through the constant A_{λ_1}. Hence the appearance of corner eddies in the present case depends upon the wedge angle α and the relative dominance of the first eigenfunction with respect to the particular solution ψ_p.

3. The sector with isothermal radial boundaries

As an illustration of the above ideas we consider, specifically, the fluid-filled sector of opening angle α with adiabatic circumferential boundary at $\bar{r} = R$ and isothermal radial boundaries at temperatures $\bar{T}_h$ and $\bar{T}_c$ corresponding to $\theta = \frac{1}{2}\alpha$ and $-\frac{1}{2}\alpha$, respectively. Then, with $\gamma = \bar{T}_h - \bar{T}_c$ and $\bar{T}_0 = \bar{T}_c$ the thermal conditions become

$$T(r, \tfrac{1}{2}\alpha) = 1, \quad T(r, -\tfrac{1}{2}\alpha) = 0, \quad \frac{\partial T}{\partial r}(1, \theta) = 0. \tag{3.1}$$

This set of conditions results in an unbounded energy flow at the wedge vertex and hence is non-physical, but nevertheless serves well for a study of the fluid motion (cf. §3.5). A similar system was considered by Liu & Joseph (1977) in which the rigid boundary $r = 1$ is replaced by a free liquid surface. In that study the shape of the liquid surface was determined as part of the analysis while special attention was given to opening angles in the range $\frac{1}{2}\pi \geqslant \alpha > 0$ for which corner eddies do not appear for the stated heating conditions.

3.1. *A particular solution*

The temperature field which satisfies (2.1) and the conditions (3.1) is independent of r:

$$T = (\theta + \tfrac{1}{2}\alpha)/\alpha. \tag{3.2}$$

Introducing (3.2) in (2.4) yields

$$\nabla^4\psi = \frac{-\cos\theta}{r\alpha}. \tag{3.3}$$

Substitution of the trial particular solution

$$\psi_p = r^3 H(\theta)$$

in (3.3) and noting the conditions

$$\psi_p(r, \pm\tfrac{1}{2}\alpha) = \frac{\partial\psi_p}{\partial\theta}(r, \pm\tfrac{1}{2}\alpha) = 0$$

on the radial surfaces yields

$$\psi_p = r^3[B\cos\theta + D\cos 3\theta - \frac{\theta}{16\alpha}\sin\theta], \tag{3.4}$$

where

$$D = -\frac{(\alpha+\sin\alpha)}{256\alpha\cos^3(\tfrac{1}{2}\alpha)\sin(\tfrac{1}{2}\alpha)}, \tag{3.5}$$

$$B = \frac{(\frac{1}{32})\sin(\frac{1}{2}\alpha) - D\cos(\frac{3}{2}\alpha)}{\cos(\frac{1}{2}\alpha)}. \tag{3.6}$$

3.2. *Corner eddies*

Since $\psi_p = O(r^3)$ it follows from (2.13) that corner eddies may exist for the present heating conditions for wedge opening angles $\alpha(<\alpha_1)$ such that $\lambda_{1r} < 2$. From (2.8) it is easily shown that the critical angle corresponding to $\lambda_{1r} = 2$, $\alpha = \alpha_2$, say, is given by the equations

$$\sin(2\alpha_2)\cosh(\lambda_{1i}\alpha_2) = -2\sin\alpha_2,$$
$$\cos(2\alpha_2)\sinh(\lambda_{1i}\alpha_2) = -\lambda_{1i}\sin\alpha_2.$$

From these equations one calculates

$$\alpha_2 \approx 126°, \quad \lambda_{1i} \approx 0.506.$$

It is clear then that in the present circumstance corner eddies may appear for opening angles in the approximate range $126° \lesssim \alpha \lesssim 146°$. Eddies certainly will exist within this range provided that the conditions on $r = 1$, (2.6), do not result in the vanishing of the coefficient A_{λ_1}. If $A_{\lambda_1} = 0$ corner eddies will not appear since $\lambda_{nr} > 2$ $(n > 1)$ for all wedge angles in the range of interest, cf. Lugt & Schwiderski (1965). It is noted that thermal conditions different from (3.1) may lead to a quite different wedge-angle range for the appearance of eddies, or no eddies at all. For example, if the boundary $\theta = \frac{1}{2}\alpha$ is heated uniformly with a flux q along its length and a sinusoidal variation of temperature is imposed on $\bar{r} = R$ it is easy to show that in this case

$$\frac{\bar{T}-\bar{T}_c}{(qR/k)} = \frac{r(\sin(\theta+\frac{1}{2}\alpha))}{\cos\alpha}, \quad \alpha < \tfrac{1}{2}\pi,$$

where k is the fluid thermal conductivity. The particular solution is then of the form

$$\psi_p = r^4\zeta(\theta), \quad \alpha < \tfrac{1}{2}\pi.$$

In this case corner eddies may be observed for values of α with $\lambda_{1r} < 3$ corresponding to wedge angles only slightly greater than 80°.

3.3. *Singular behaviour for* $\alpha = \pi$

The particular case $\alpha = \pi$, corresponding to a semicircular duct is of special interest. It is shown by Lugt & Schwiderski (1965) that, as α approaches π, increasing numbers of (leading) eigenvalues $\lambda_1, \lambda_2 \ldots$ are real-valued. Hence for α near π

$$\psi = \psi_{\mathrm{p}} + A_{\lambda_1}\psi_{\lambda_1} + A_{\lambda_2}\psi_{\lambda_2} + \ldots,$$

where the λ_n, A_{λ_n} and ψ_{λ_n} are real. For $\alpha = \pi$ all eigenvalues are real and

$$\lambda_n = n, \quad n = 1, 2, 3 \ldots.$$

The eigenfunctions are then

$$\psi_{\lambda_n} = r^{n+1}\{\cos[(n+1)\theta] + q_n \cos[(n-1)\theta]\},$$

where

$$q_n = -\lim_{\alpha\to\pi} \frac{\cos[(\lambda_n+1)\tfrac{1}{2}\alpha]}{\cos[(\lambda_n-1)\tfrac{1}{2}\alpha]} = \begin{cases} 1, & n = 1, 3, 5 \ldots \\ \dfrac{n+1}{n-1}, & n = 2, 4, 6 \ldots \end{cases}.$$

Note, however, that the coefficients in the particular solution (B and D in (3.5) and (3.6)) become unbounded in the limit $\alpha \to \pi$. Such unexpected singular behaviour at one or more isolated values of the wedge angle α has been observed before in various physical contexts, see for example Sternberg & Koiter (1958), Dempsey (1981) and Ting (1984). Moffatt & Duffy (1980) obtain bounded results for Poiseuille flow in a duct whose cross-section has a sharp corner by simply noting that the singular portion of the particular solution at the critical angle is compensated for by one or more components of the eigenfunction series. A similar approach was taken by Ting (1984, 1985) and will be adopted here.

Near $\alpha = \pi$ we take

$$\psi = \psi_{\mathrm{p}} + C(\alpha)\psi_{\lambda_2} + \sum_n A_{\lambda_n}\psi_{\lambda_n}, \tag{3.7}$$

where we have appended to the right-hand side of (2.10), without loss of generality, the second eigenfunction ψ_{λ_2} (which is $O(r^3)$ in the limit $\alpha \to \pi$) with the α-dependent multiplier $C(\alpha)$. The function $C(\alpha)$ is constructed so that

$$\lim_{\alpha\to\pi} |\psi_{\mathrm{p}} + C(\alpha)\psi_{\lambda_2}| < \infty. \tag{3.8}$$

Expanding ψ_{p} and ψ_{λ_2},

$$\psi_{\mathrm{p}} = r^3\{\tfrac{1}{32}[3\cos\theta + \cos 3\theta](\alpha-\pi)^{-3} + \tfrac{1}{128}[\cos 3\theta - 9\cos\theta](\alpha-\pi)^{-1}$$

$$+ \frac{1}{16\pi}[\tfrac{1}{12}\cos 3\theta - \tfrac{3}{4}\cos\theta - \theta\sin\theta] + O(\alpha-\pi)\}, \quad \alpha \to \pi, \tag{3.9}$$

$$\psi_{\lambda_2} = r^3\{\cos 3\theta + 3\cos\theta - 3\cos\theta(\alpha-\pi)^2 + \frac{1}{\pi}[(\cos 3\theta$$

$$+ 3\cos\theta)\log r - 2\cos\theta - \theta\sin 3\theta - 3\theta\sin\theta](\alpha-\pi)^3 + O(\alpha-\pi)^4\}, \quad \alpha \to \pi. \tag{3.10}$$

Let

$$C(\alpha) = C_3(\alpha-\pi)^{-3} + C_2(\alpha-\pi)^{-2} + C_1(\alpha-\pi)^{-1}, \quad \alpha \to \pi, \tag{3.11}$$

where C_1, C_2 and C_3 are constants to be determined by (3.8). Substituting (3.9), (3.10) and (3.11) in (3.8) we obtain

$$C_1 = -\tfrac{1}{128}, \quad C_2 = 0, \quad C_3 = -\tfrac{1}{32}.$$

Hence the *modified* particular solution, $\tilde{\psi}_p$, corresponding to the special case $\alpha = \pi$ is

$$\lim_{\alpha \to \pi} (\psi_p + C(\alpha)\psi_{\lambda_2}) = \frac{r^3}{32\pi}\{(\tfrac{1}{6} - \log r)[\cos 3\theta + 3\cos\theta] + \theta[\sin 3\theta + \sin\theta]\}$$

or

$$\tilde{\psi}_p = \frac{1}{32\pi}\{[\tfrac{1}{6} - \log r]\,\psi_{\lambda_2} + r^3\,\theta[\sin 3\theta + \sin\theta]\}.$$

It can be easily shown that $\tilde{\psi}_p$ satisfies (3.3) along with the conditions on the radial boundaries for $\alpha = \pi$ and hence is a bounded particular solution and replaces (3.4) in this special case.

3.4. *Evaluation of the* A_{λ_n}

The stream function in the sector is given by

$$\psi = \psi_p + \sum_n A_{\lambda_n}\psi_{\lambda_n}, \tag{3.12}$$

where for complex λ_n, the real part of the terms $A_{\lambda_n}\psi_{\lambda_n}$ is understood. If λ_k is complex then the corresponding term in (3.12) is of the form

$$\mathrm{Re}\{A_{\lambda_k}\psi_{\lambda_k}\} = E_k\,\mathrm{Re}\{\psi_{\lambda_k}\} + F_k\,\mathrm{Im}\{\psi_{\lambda_k}\},$$

where E_k and F_k are real-valued constants. In any case, the constants are determined by the condition of zero velocity on the circumferential boundary, $r = 1$,

$$0 = \psi_p(1,\theta) + \sum_n A_{\lambda_n}\psi_{\lambda_n}(1,\theta), \tag{3.13}$$

$$0 = \frac{\partial\psi_p}{\partial r}(1,\theta) + \sum_n A_{\lambda_n}\frac{\partial\psi_{\lambda_n}}{\partial r}(1,\theta). \tag{3.14}$$

In the study of Liu & Joseph (1977) the eigenfunctions (2.7), with the λ_n from (2.8), are used to generate biorthogonal series, the properties of which are exploited for the direct computation of the constants. The conditions on $r = 1$ in the reference configuration used by Liu & Joseph are of course the ones appropriate to a free liquid surface and as such are quite distinct from (3.13) and (3.14). Here we use a simple alternative approach for the determination of the A_{λ_n} suggested by Carrier & Shaw (1950). The (even) functions on the right-hand side of (3.13) and (3.14) are made orthogonal to the functions $\cos(2k\pi\theta/\alpha)$ on the interval $-\frac{1}{2}\alpha < \theta < \frac{1}{2}\alpha$ by appropriate choice of the constants A_{λ_n} (or E_n and F_n as the case may be), i.e.

$$\int_0^{\frac{1}{2}\alpha}[\psi_p(1,\theta) + \sum_n A_{\lambda_n}\psi_{\lambda_n}(1,\theta)]\cos\frac{2k\pi\theta}{\alpha}\,\mathrm{d}\theta = 0, \quad k = 0, 1, 2\ldots,$$

$$\int_0^{\frac{1}{2}\alpha}\left[\frac{\partial\psi_p}{\partial r}(1,\theta) + \sum_n A_{\lambda_n}\frac{\partial\psi_{\lambda_n}}{\partial r}(1,\theta)\right]\cos\frac{2k\pi\theta}{\alpha}\,\mathrm{d}\theta = 0, \quad k = 0, 1, 2\ldots.$$

The infinite system that results for the A_{λ_n} is truncated such that the conditions

$$\max|\psi(1,\theta)|/|\psi_{\max}(r,\theta)| < 10^{-2},$$

$$\max\left|\frac{\partial\psi}{\partial r}(1,\theta)\right| \Big/ \left|\left[\frac{\partial\psi}{\partial r}(r,\theta)\right]_{\max}\right| < 10^{-2}$$

n	$E_n \times 10^5$	$F_n \times 10^5$
1	8580	2916
2	42.11	49.05
3	−10.10	0.1853
4	2.822	−1.423
5	−0.9455	0.8742
6	0.3571	−0.4950
7	−0.1454	0.2850
8	0.06278	0.1682
9	−0.03280	0.09946
10	0.04523	−0.06009
11	−0.01494	0.2001

TABLE 1. E_n and F_n for $\alpha = 120°$

are satisfied where $\psi_{\max}(r, \theta)$ and $[(\partial\psi/\partial r)(r, \theta)]_{\max}$ denote the maximum values of the stream function and u_θ in the sector. It was found that in the range $0 < \alpha \leqslant \pi$ investigated here, no more than sixteen terms in the expansion (3.12) were required. Table 1 lists the constants E_n, F_n for the case $\alpha = 120°$.

3.5. *Relevance to the case of 'almost isothermal' radial boundaries*

The present thermal boundary conditions (3.1), as noted earlier, are non-physical owing to the unbounded energy flow at the wedge vertex. It is appropriate here to comment on the physical relevance of the wedge flow which evolves from these non-physical thermal conditions. We demonstrate below that the motion in the wedge is altered, to only a negligible extent over most of the wedge volume, when the present (singular) thermal conditions are replaced by physically realizable conditions differing from those of (3.1) only in a small neighbourhood of the vertex. It is sufficient to consider the *partial* sector of opening angle α with insulated circumferential boundaries $r = 1$ and $r = \epsilon$ ($\ll 1$) and isothermal radial surfaces, $T(r, \frac{1}{2}\alpha) = 1$, $T(r, -\frac{1}{2}\alpha) = 0$. This sectorial region differs from the full sector only by the small 'cutout' vertex region of dimension ϵ. Clearly, energy flow in this slightly perturbed domain is bounded. Temperature, T, and ψ_{p} in the partial sector are still given by (3.2) and (3.4)–(3.6), respectively; however, to the expression for ψ, (2.10), we must append the symmetric biharmonic functions

$$r^{1-\lambda_n} C_{\lambda_n}(\theta),$$

where $C_{\lambda_n}(\theta)$ corresponds to the bracketed part of (2.7) and the parameters λ_n are given by (2.8) as before. The full expression for ψ in the partial sector is then

$$\psi = \psi_{\mathrm{p}} + \sum_n [A_{\lambda_n} r^{1+\lambda_n} + B_{\lambda_n} r^{1-\lambda_n}] C_{\lambda_n}(\theta). \tag{3.15}$$

Note that the constants B_{λ_n} are suppressed in the case of the full sector in order to satisfy the no-slip condition at the vertex. Formally, the constants A_{λ_n} and B_{λ_n} in (3.15) are determined by the condition of zero fluid velocity on the two circumferential boundaries, $r = \epsilon, 1$. However, it is only necessary here to consider the condition $\psi(\epsilon, \theta) = 0$, i.e.

$$-\psi_{\mathrm{p}}(\epsilon, \theta) = \sum_n [A_{\lambda_n} \epsilon^{1+\lambda_n} + B_{\lambda_n} \epsilon^{1-\lambda_n}] C_{\lambda_n}(\theta). \tag{3.16}$$

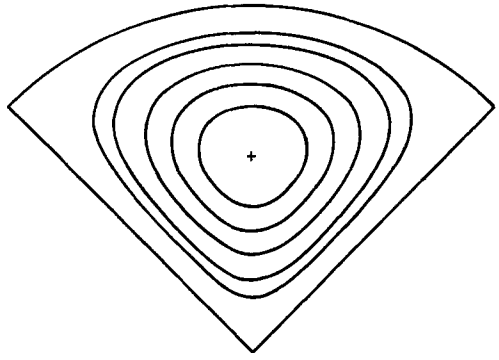

FIGURE 2. Stream function contours $\psi/\psi_{\max} = 0.1, 0.2, 0.4, 0.6, 0.8$ with $\psi_{\max} = -7.36 \times 10^{-4}$ for the sector with no-slip boundary ($r = 1$) and $\alpha = 90°$.

Note that the magnitude $|\epsilon^{1-\lambda_n}| = \epsilon^{1-\lambda_{nr}}$ and recall that $\lambda_{nr} > 1$ for the range of α under consideration (cf. Lugt & Schwiderski 1965) and that $\psi_p(\epsilon, \theta) = O(\epsilon^3)$. It follows then from (3.16) that in the limit as the partial sector is made to approach the full sector geometry, i.e. as $\epsilon \to 0$

$$|B_{\lambda_n}| = o(\epsilon^{\lambda_{nr}-1})$$

No such restriction is in effect for the A_{λ_n} and therefore we expect the A_{λ_n} to behave in a regular manner in this limit and smoothly approach the values appropriate for the full sector ($\epsilon = 0$). Clearly then, in the 'almost singular' case $\epsilon \ll 1$, the terms $B_{\lambda_n} r^{1-\lambda_n}$ make a negligible contribution to the sum in (3.15) except perhaps in the immediate vicinity of the boundary $r = \epsilon$. This insensitivity of the global motion to alterations in conditions over a portion of the boundary is also predicted by direct consideration of the systems for T and ψ, i.e. (2.1) and (2.4) along with their respective boundary conditions. These systems have direct analogues in the theory of elastostatics. For example, the system governing T also governs the out-of-plane displacement in an elastic wedge with uniform displacement specified along the radial boundaries when the circumferential surface $r = 1$ is traction-free. In such cases Saint-Venant's Principle asserts that the effect of stresses applied over a portion of the boundary of a body is negligible at distances that are large compared with the linear dimension of that boundary portion (cf. Boussinesq 1885). Hence, in the present circumstance it is anticipated that alteration of the thermal conditions over a small section of the wedge boundary of dimension ϵ about the wedge vertex (i.e. the case of almost isothermal radial boundaries) will affect the resulting motion to a negligible degree except in the small neighbourhood of dimension ϵ about $r = 0$.

3.6. *Results*

Contours of ψ for $\alpha = 90°$ are plotted in figures 2 and 3. The contours of figure 3 correspond to a condition of zero shear stress on the circular boundary $r = 1$, that is, the condition

$$\frac{\partial u_\theta}{\partial r}(1, \theta) = \frac{\partial^2 \psi}{\partial r^2}(1, \theta) = 0 \tag{3.17}$$

replaces the second part of (2.6). Note that in each case the motion in the sector is unicellular with warmer fluid flowing radially outward (ascending) along the heated surface and cooler fluid flowing radially inward (descending) along the cooled boundary. Corner eddies are absent from the flow as predicted in the discussion of §3.2. Comparison of figures 2 and 3 indicates that the shear-free condition (3.17) leads

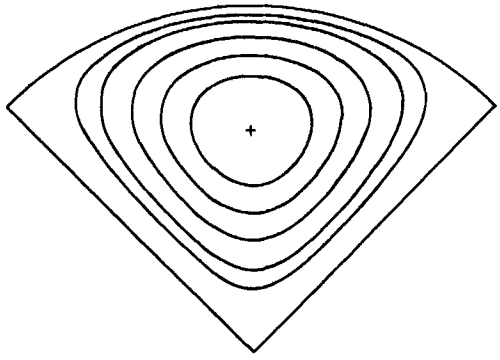

FIGURE 3. Stream function contours $\psi/\psi_{max} = 0.1, 0.2, 0.4, 0.6, 0.8$ with $\psi_{max} = -1.14 \times 10^{-3}$ for the sector with shear-free boundary ($r = 1$) and $\alpha = 90°$.

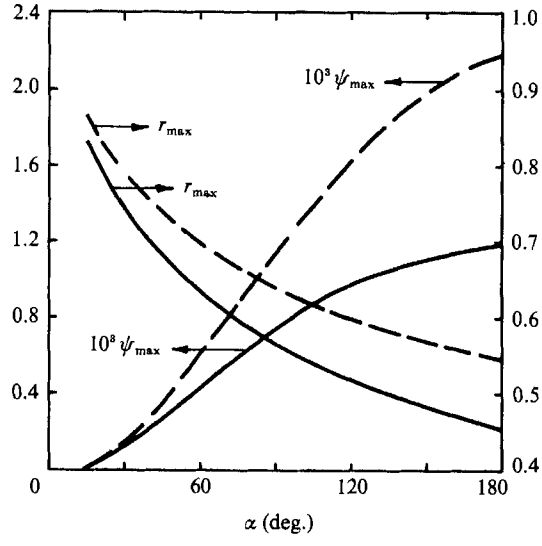

FIGURE 4. Variation of the maximum stream function, ψ_{max}, and the location of the maximum stream function, r_{max}, with wedge angle α for no-slip (——) and shear-free (– – –) conditions on $r = 1$.

to more intense circulation in the sector. Also, the maximum value of the stream function ψ_{max} occurs at a distance from the sector vertex, r_{max}, that is greater than for the no-slip case. This is to be expected as the quenching effect on the flow due to the no-slip condition on the boundary $r = 1$ is absent in figure 3. This behaviour was evident for all wedge angles; however, the distinction between the no-slip and shear-free cases diminishes with decreasing α since the circumferential boundary represents a smaller proportion of the complete sector boundary for small α. This effect is shown clearly in figure 4 in which the value of the maximum stream function, ψ_{max}, and its radial position in the sector, r_{max}, are plotted versus wedge angle in the range $0 < \alpha \leqslant \pi$ for both the no-slip and shear-free cases. From this figure it is also clear that the radial boundaries strongly attenuate the circulation as α is decreased. At the same time, the centre of the cell moves away from the vertex, toward the upper portion of the sector where the influence of the converging radial surfaces is least.

The radial velocity distribution at the location $r = r_{max}$ is plotted as a function of θ/α for the opening angles $\alpha = 60°$, $80°$, $120°$, $160°$ and $180°$ in figure 5. It is evident

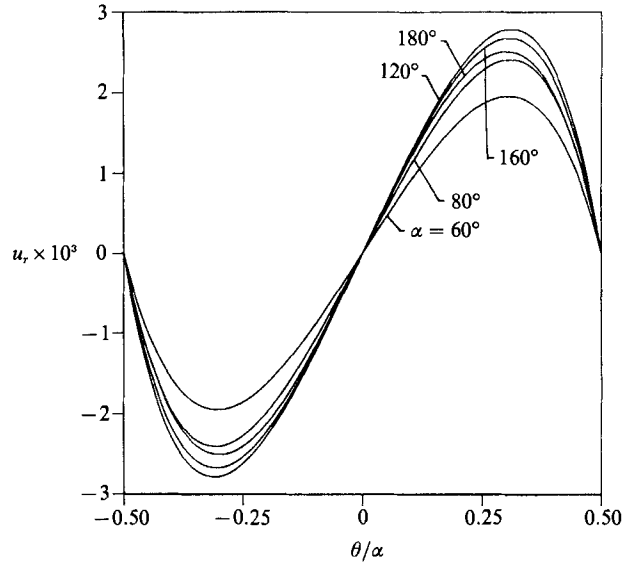

FIGURE 5. Distribution of radial velocity, u_r, along $r = r_{max}$, no-slip on $r = 1$.

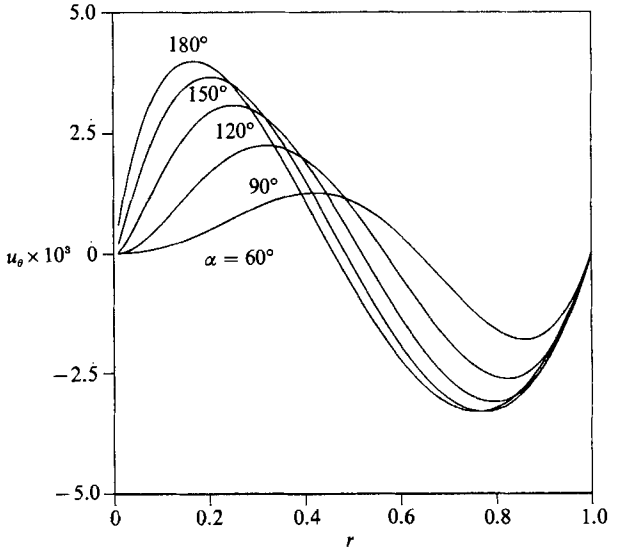

FIGURE 6. Distribution of circumferential velocity, u_θ, along the radius $\theta = 0$, no-slip on $r = 1$.

from this figure that the radial velocity does not increase monotonically with increasing α. As the wedge angle increases from acute values the radial velocity increases owing to the lessening effect of viscous resistance. This throttling of the flow (for small α) comes about as a consequence of the symmetric counterflow between the two radial surfaces. On the other hand, as the wedge angle increases further, becoming more obtuse, isotherms in the sector are less-closely spaced (equation (3.2)) and on average are not closely aligned with the gravity vector. The driving force for the motion, i.e. the right-hand side of (3.3), is therefore diminished and the radial velocity in the sector falls off slightly with increasing α in the range $120° \lesssim \alpha \lesssim 180°$ as shown in figure 5. The magnitude of the velocity component u_θ, figure 6, increases steadily with α. Peak circumferential velocity is found on the vertex side of the cell

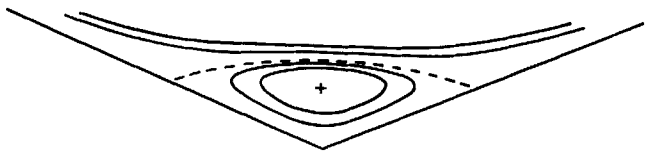

FIGURE 7. Stream function contours $\psi/\psi' = -2, -1, 0, 0.4, 0.5$ in the vicinity of the vertex showing the first corner eddy for the case $\alpha = 135°$ with no-slip on $r = 1$. The maximum stream function value for the first eddy is $\psi' = 9.06 \times 10^{-19}$.

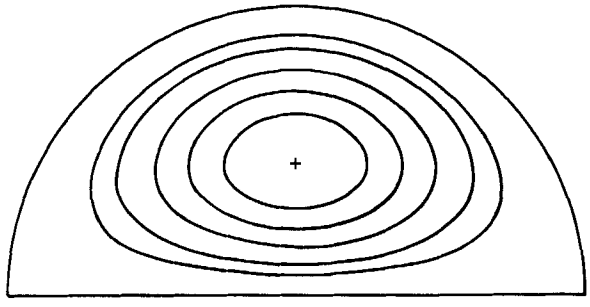

FIGURE 8. Stream function contours $\psi/\psi_{max} = 0.1, 0.2, 0.4, 0.6, 0.8$ with $\psi_{max} = -1.18 \times 10^{-3}$ for the sector with no-slip boundary ($r = 1$) and $\alpha = 180°$.

centre location $r = r_{max}$ for larger wedge angles, $\alpha \gtrsim 120°$. For decreasing opening angles the centre of the cell moves toward larger values of r (cf. figure 4) and hence peak values of u_θ occur nearer to the circumferential boundary of the sector.

The first corner eddy for the case $\alpha = 135°$ is shown in figure 7. Only the single corner eddy shown may be depicted in this figure (aside from a small portion of the main cell) since the dimension of consecutive eddies decreases quite rapidly for $\alpha = 135°$. It is demonstrated by Moffatt (1964) that the ratio of dimensions of any two consecutive eddies is approximately e^9 for the case $\alpha = 135°$ and the strength of consecutive eddies falls off even more rapidly. In figure 7 the approximate location of the zero streamline separating the main cell from the first corner eddy is given by $r = 2 \times 10^{-6}$ at $\theta = 0$ while the circulation strength of the first eddy and the main cell are separated by more than 15 orders of magnitude. It is of interest to note that within the eddy region the motion is exactly counter, in a rotational sense, to what would be anticipated by consideration of the local density field alone. That is, less-dense fluid falls adjacent to the warmer radial surface while more-dense fluid rises adjacent to the cooled surface. This circulation pattern, however, seems quite natural if it is recalled that the most dominant eigenmotion is not driven by buoyant effects but instead arises as a consequence of the minimization of local energy dissipation subject to the driving shear of the main (buoyancy-driven) cell.

The case $\alpha = \pi$, figure 8, corresponds to a semicircular duct heated over one half and cooled over the other half of the plane boundary. Less-dense fluid in the left portion ($\theta > 0$) of the sector is displaced by heavier, cooler fluid from the right-hand portion ($\theta < 0$) moving across the lower surface $\theta = \pm\frac{1}{2}\alpha$.

The authors wish to acknowledge the many helpful suggestions and alternative points of view offered by Professor J. L. Bassani during the course of this work.

REFERENCES

BATCHELOR, G. K. 1967 *An Introduction to Fluid Dynamics*. Cambridge University Press.
BOUSSINESQ, M. J. 1885 *Application des Potentiels*. Gauthier-Villars.
CARRIER, G. F. & SHAW, F. S. 1950 *Proc. Symp. Appl. Maths* **3**, 125.
DEMPSEY, J. P. 1981 *J. Elasticity* **11**, 1.
JEFFREY, D. J. & SHERWOOD, J. D. 1980 *J. Fluid Mech.* **96**, 315.
LIU, C. H. & JOSEPH, D. D. 1977 *J. Fluid Mech.* **80**, 443.
LUGT, H. J. & SCHWIDERSKI, E. W. 1965 *Proc. R. Soc. Lond.* A**285**, 382.
MOFFATT, H. K. 1964 *J. Fluid Mech.* **18**, 1.
MOFFATT, H. K. & DUFFY, B. R. 1980 *J. Fluid Mech.* **96**, 299.
STERNBERG, E. & KOITER, W. T. 1958 *Trans. ASME* E: *J. Appl. Mech.* **25**, 575.
TING, T. C. T. 1984 *J. Elasticity* **14**, 235.
TING, T. C. T. 1985 *Q. J. Mech. Appl. Maths* **38**, 245.